Binding free energy and counterion release for adsorption of the antimicrobial peptide lactoferricin B on a POPG membrane

Igor S. Tolokh*
Department of Physics, University of Guelph, Guelph, Ontario, Canada N1G2W1

Victor Vivcharuk†
Biophysics Interdepartmental Group and Department of Physics, University of Guelph, Guelph, Ontario, Canada N1G2W1

Bruno Tomberli‡
Department of Physics and Astronomy, Brandon University, Brandon, Manitoba, Canada R7A 6A9

C. G. Gray§
Guelph-Waterloo Physics Institute and Department of Physics, University of Guelph, Guelph, Ontario, Canada N1G2W1
(Received 5 October 2008; revised manuscript received 28 May 2009; published 22 September 2009)

Molecular dynamics (MD) simulations are used to study the interaction of an anionic palmitoyl-oleoyl-phosphatidylglycerol (POPG) bilayer with the cationic antimicrobial peptide bovine lactoferricin (LFCinB) in a 100 mM NaCl solution at 310 K. The interaction of LFCinB with a POPG bilayer is employed as a model system for studying the details of membrane adsorption selectivity of cationic antimicrobial peptides. Seventy eight 4 ns MD production run trajectories of the equilibrated system, with six restrained orientations of LFCinB at 13 different separations from the POPG membrane, are generated to determine the free energy profile for the peptide as a function of the distance between LFCinB and the membrane surface. To calculate the profile for this relatively large system, a variant of constrained MD and thermodynamic integration is used. A simplified method for relating the free energy profile to the LFCinB-POPG membrane binding constant is employed to predict a free energy of adsorption of -5.4 ± 1.3 kcal/mol and a corresponding maximum adsorption binding force of about 58 pN. We analyze the results using Poisson-Boltzmann theory. We find the peptide-membrane attraction to be dominated by the entropy increase due to the release of counterions and polarized water from the region between the charged membrane and peptide, as the two approach each other. We contrast these results with those found earlier for adsorption of LFCinB on the mammalianlike palmitoyl-oleoyl-phosphatidylcholine membrane.

DOI: 10.1103/PhysRevE.80.031911 PACS number(s): 87.15.A−, 87.15.B−

I. INTRODUCTION

The interaction of cationic antimicrobial peptides (CAPs) [1] with the surfaces of bacterial and eukaryotic cell membranes is of importance in many technical and biological processes, especially for designing peptides which can modulate cell membrane properties. Antimicrobial peptides have demonstrated antibacterial, antiviral, and antifungal activities. They have the ability to kill Gram-negative and Gram-positive bacteria, mycobacteria, enveloped viruses, fungi, and even transformed or cancerous cells. They may have a direct effect, but they also appear to be broadly involved in the activation of the innate immune system and inflammatory responses (see review in [2]).

In a previous paper [3] we carried out a simulation study of bovine lactoferricin (LFCinB) [4] interacting with an uncharged mammalianlike membrane, i.e., palmitoyl-oleoyl-phosphatidylcholine (POPC) bilayer. The current simulation study, LFCinB interacting with the charged bacterial-like palmitoyl-oleoyl-phosphatidylglycerol (POPG) membrane, shows a dramatic difference in binding. We discuss the importance of and physical reasons for this difference. One of the most basic models that explains the ability of most antimicrobial peptides to distinguish prokaryotic from eukaryotic cells is based on the differences in macromolecular constitution, structure, and charge distribution of prokaryotic and eukaryotic membranes. The outer leaflet of mammalian cell plasma membranes mainly comprises neutral phosphatidylcholine (PC), phosphatidylethanolamine, sphingomyelin, and cholesterol lipids [5]. In contrast, cytoplasmic bacterial membranes contain significant amounts of negatively charged phosphatidylglycerol (PG) and cardiolipin (CL) lipids [6]. Gram-positive bacteria have only a cytoplasmic membrane, but Gram-negative bacteria have both a cytoplasmic or inner membrane and an outer membrane. For both Gram-positive and Gram-negative bacteria, the limited available evidence [6] suggests that the outer leaflet of the cytoplasmic membrane has PG and CL lipids. For one specific Gram-positive bacterium 60% of the PG has been shown to be in the outer leaflet [7]. For Gram-negative bacteria, the outer leaflet of the outer membrane has, in addition, negatively charged lipopolysaccharide (LPS) attached to it. We

*tolokh@physics.uoguelph.ca
†Corresponding author. Present address: Department of Chemical Engineering and Materials Science, University of Minnesota, Minneapolis, MN 55455-0132, USA; vivch001@umn.edu
‡tomberlib@brandonu.ca
§cgg@physics.uoguelph.ca

defer discussion of membranes with attached LPS to future work. Another strong difference between membranes of prokaryotic and eukaryotic cells is that bacterial cells have a larger transmembrane potential [8,9]. This difference has been hypothesized and also of importance for the selectivity of CAPs [10].

Many hypotheses have been presented to describe the antimicrobial activity of CAPs [1,2,11]. For example, in Gram-negative bacteria the CAP interaction with an outer membrane occurs through electrostatic binding between the cationic peptide and the negatively charged LPSs. This leads to a disturbance of the outer membrane structure. It has been shown [9,12,13] that the possible mechanism of action for some CAPs is to bind to LPS and degrade the outer membrane by replacing divalent cationic ions which normally function as cationic bridges between adjacent phosphate groups of LPS. Once this occurs, the peptides can translocate across the outer membrane to the negatively charged cytoplasmic membrane. The relatively high concentration of anionic lipids (PG and CL) in this membrane plays an important role in the selectivity of a CAP for bacterial cells over eukaryotic cells [8].

As a result of strong interaction with bacterial membranes, the peptides can permeabilize the membranes causing cell lysis. It has been suggested that most CAPs bind to and perturb the cytoplasmic membrane thus causing a fatal depolarization of the bacterial membrane [14], creating physical holes that cause cellular contents to leak out [15]. It is also well established that some peptides do not cause membrane permeabilization and can translocate across the membrane into the cytoplasm without membrane disruption yet still cause bacterial cell death. After penetrating into the cell, peptides damage important intracellular targets. They cause inhibition of nucleic acid synthesis, protein synthesis, enzymatic activity, and cell wall synthesis [16–18].

Regardless of their precise mode of action, the activities of antimicrobial peptides are dependent on interaction with bacterial cell membranes because even CAPs that attack intracellular targets must pass through the bacterial membrane. CAP interactions and their selectivity with real membranes are poorly understood. Therefore studies with model membranes clearly provide important information about mechanisms of interaction of CAPs with target bacterial membranes. The mechanics of this process is still unknown at the molecular level.

In this paper we investigate the interaction of LFCinB with an anionic POPG membrane since PG lipids are one of the major constituents of bacterial membranes. We compare our results with our previous ones obtained for a neutral POPC membrane [3], chosen as a model for eukaryotic cell plasma membranes. We also restrict ourselves to surface (or adsorption) interactions. Subsequent work will expand current understanding by considering peptide penetration into POPC, POPG, and mixed POPG/POPC membranes.

The membrane-peptide binding thermodynamics formalism together with the algorithm for obtaining the potential of mean force (PMF) for adsorption [3] is briefly summarized in Sec. II. We express the adsorption observables in terms of the single-molecule PMFs, $W(z,\Omega)$ and $W(z)$. Here $W(z,\Omega)$ is the orientation-dependent PMF and $W(z)$ is the orientation-averaged PMF. Section III contains some computational details and the molecular dynamics (MD) protocol used for the LFCinB-POPG simulation. In Sec. IV we apply our algorithm [3] to calculate the PMFs for the LFCinB-POPG system. From the PMFs we predict the standard free energy for the LFCinB adsorption on a POPG membrane. In Sec. V we compare the MD results for the PMF with results obtained from Poisson-Boltzmann (PB) theory. We use this theory to analyze the electrostatic entropic and enthalpic contributions to the free energy based on the concepts of counterion release from the ionic double layers and the entropy increase due to the release of polarized water molecules between the peptide and membrane, as the two approach each other. Conclusions follow in Sec. VI.

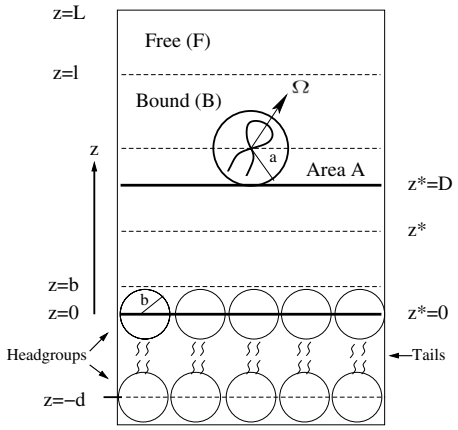

FIG. 1. Schematic binding geometry of the peptide at the POPG membrane surface and simplified geometry for PB analysis. The box length in the z direction is approximately L and the area of the xy plane in the transverse direction is A. The peptide configuration is defined by a center of mass z-coordinate z and orientation Ω. There are $N=N_F+N_B$ peptides in volume $V\simeq LA=V_F+V_B$, where $z=l$ divides the free (F) and bound (B) volumes. For the purpose of defining a distance of closest approach l', the POPG head groups can be represented by spheres with effective radius $b\approx 4$ Å and $l'=a+b$ defines an effective excluded volume (Al'), with a given below. The distance $d=36.3$ Å is the mean distance between the head group phosphorus atoms in the two membrane leaflets. For the PB analysis two simplified geometries are used. The first is a sphere-plane geometry with $a\approx 10$ Å as the radius of the sphere representing the peptide. The second is a plane-plane geometry, representing two oppositely charged planar surfaces, with charge densities σ_+ and σ_-, separated by distance D. z^* is the running coordinate between the two surfaces for the reduced electrical potential $\phi(z^*)$, as explained in the text. The origin $z=0$ ($z^*=0$) is chosen at the membrane surface (average position of the upper leaflet phosphorus atoms).

II. THEORY

In this section we briefly summarize some results from our earlier paper [3]. Consider the schematic binding geometry of Fig. 1. For the simulation we consider all-atom models for the peptide (shown schematically as a twisted hairpin in Fig. 1), membrane, water, and ions. We consider a dilute solution of N identical peptides in a solution of Na^+, Cl^- ions

at temperature T and volume $V \simeq AL$ (see Fig. 1). The number of Na^+ and Cl^- ions is chosen such that the whole system is net neutral. The coordinate z is the normal coordinate of the center of mass of a peptide, with $z=0$ chosen as the average position of the upper leaflet phosphorus atoms of the membrane lipids. Ω denotes the peptide orientation. Peptides are considered to be bound (B) if $z<l$ and free (F) if $z>l$, where the determination of l is discussed in [3]. The densities of bound and free peptide are $\rho_B=N_B/V_B$ and $\rho_F=N_F/V_F$, respectively, where $V_B=A(l-l')$ and $V_F=A(L-l)\approx AL\simeq V$ since $l \ll L$ and l' defines an effective excluded volume (Al') which is related to the size of the peptide and the choice of $z=0$ (see Fig. 1 caption). In Sec. VI we introduce simplified geometries, also shown in Fig. 1, in order to do a PB analysis of the peptide-membrane interaction. For this analysis the membrane is considered as a uniformly negatively charged plane, and the peptide is considered as a positively charged sphere and, in an even more simplified model, as a positively charged plane. The water is taken to be a dielectric continuum and the ions as continuous charge distributions.

To compute the orientation-dependent PMF $W(z,\Omega)$ from the simulation, we employ the force method we developed for the PMF calculation of LFCinB in the vicinity of a neutral membrane [3]; it is a variant of constrained MD and thermodynamic integration [19–24]. For obtaining $W(z,\Omega)$ we use the relation $\bar{F}(z,\Omega)=-\partial W(z,\Omega)/\partial z$, where $\bar{F}(z,\Omega)$ is the mean force (which is in z direction by symmetry) on the peptide for fixed z and Ω. In our method we replace the rigid "constraint" forces on the peptide by nonrigid (but fairly stiff) "restraint" forces $F^{res}(z,\Omega)$ using attached springs. On average, the net force $\bar{F}(z,\Omega)$ on the peptide due to the "solvent" (i.e., water, ions, and membrane) is balanced by that due to the restraints $\bar{F}^{res}(z,\Omega)$, i.e., $\bar{F}(z,\Omega)+\bar{F}^{res}(z,\Omega)=0$. In our studies both the LFCinB peptide and the membrane are restrained in space and the forces exerted on both the LFCinB and membrane harmonic restraint springs are monitored and averaged. The springs record smaller fluctuations than those of the direct forces due to the inertia of the particles attached to the springs [3]. We find the thermal fluctuations in $F^{res}(z,\Omega)$ to be approximately three to four times smaller than those in $F(z,\Omega)$. Therefore we can obtain $W(z,\Omega)$ as

$$W(z,\Omega) = -\int_{\infty}^{z} \bar{F}(z',\Omega)dz', \tag{1}$$

with $\bar{F}(z',\Omega)=-\bar{F}^{res}(z',\Omega)$.

The orientation-averaged PMF $W(z)$ is related to orientation-dependent PMF $W(z,\Omega)$ by

$$e^{-\beta W(z)} = \int \frac{d\Omega}{8\pi^2} e^{-\beta W(z,\Omega)}, \tag{2}$$

where $\beta=1/k_BT$ with k_B as Boltzmann's constant. For the peptide orientation Ω we can use, for example, three Euler angles or three Tait-Bryan angles (see Sec. IV). For calculation of the equilibrium binding constant $K=\rho_B/\rho_F$ and related adsorption free energy ΔG^0 we use [3]

$$K = \frac{1}{l-l'}\int_{l'}^{l} dz e^{-\beta W(z)} \equiv \langle e^{-\beta W}\rangle_{\Delta l} \tag{3}$$

and the standard relation

$$\Delta G^0 = -k_BT \ln K. \tag{4}$$

As in our previous paper [3] the free energy profile $W(z)$ can be decomposed into enthalpic $[\Delta H(z)]$ and entropic $[-T\Delta S(z)]$ components using

$$W(z) = \Delta H(z) - T\Delta S(z), \tag{5}$$

where

$$\Delta H(z) = \partial[\beta W(z)]/\partial\beta \tag{6}$$

and $T\Delta S(z)$ is then found from Eq. (5). However, for the LFCinB-POPG interactions discussed here, the approximation used in [3] to evaluate Eq. (6) is not valid, and $\Delta H(z)$ cannot be obtained from $W(z)$ based on MD simulations at a single temperature. Therefore, in Sec. VI, we analyze our system in terms of Poisson-Boltzmann theory. Analytical results for $W(z)$ within the PB approach allow $\Delta H(z)$ and $T\Delta S(z)$ to be calculated using Eqs. (5) and (6).

III. MD SIMULATION

A. General computational details

Our computer simulations are carried out on the multi-institutional high-performance computing network, SHARCNET [25], using the program CHARMM [26] with the CHARMM27 force field [27]. The van der Waals interactions are smoothly switched off over a distance of 4 Å, between 8 and 12 Å. The electrostatic interactions are simulated using Ewald summation with no truncation [28]. During *NVT* and *NPT* dynamics bond lengths involving hydrogen atoms are constrained with the SHAKE algorithm [29], thus allowing the use of a 2 fs time step. The temperature of the system is set to 310 K above the gel-liquid crystal phase transition of the POPG membrane. The water molecules are simulated using the TIP3P water model [30], where TIP3P is an abbreviation for "transferable intermolecular potential three point charges."

B. Microscopic models for LFCinB peptide and POPG membrane

Two simulations steps are performed to get the final system geometry shown in Fig. 2.

(i) We simulate a solvated lipid bilayer system of 128 anionic POPG lipids (i.e., 64 lipids in each leaflet) with 128 Na^+ counterions and 3527 TIP3P water molecules. Our POPG membrane simulation using the CHARMM27 force field is based on the final configuration after a 150 ns MD simulation [31,32] using the united atom force field of Berger *et al.* [33] and GROMACS software with equal numbers of two chiral isomers D-POPG and L-POPG creating a lipid bilayer system with neutral chirality [34]. After initial energy minimization using the CHARMM27 force field, the resulting POPG system is simulated for 7 ns in the isothermal-isobaric

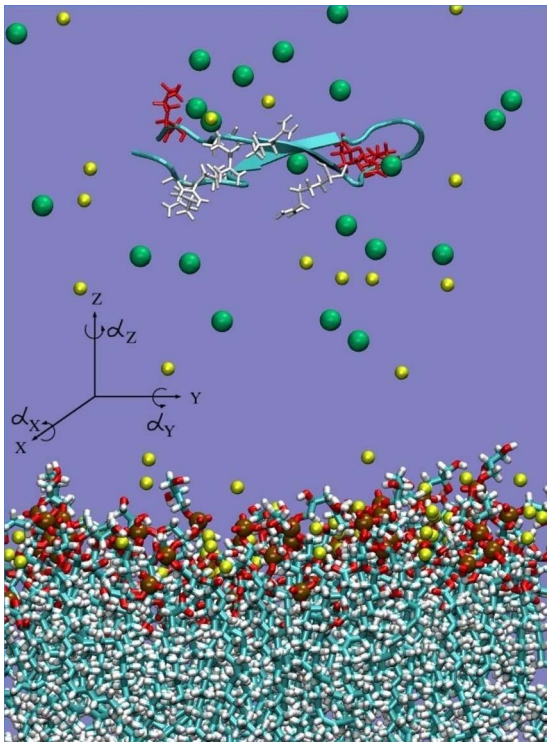

FIG. 2. (Color online) Snapshot of molecular structure showing the initial (0,0,0) orientation of the six principal orientations studied of LFCinB near the upper leaflet of the POPG membrane. The lipid head phosphorus atoms are shown as brown spheres and lipid oxygen atoms are shown in red. The solution Na^+ and Cl^- counterions are shown as small yellow and large green spheres, respectively. The peptide basic residues [i.e., five Arg (in white) and three Lys (in red)] are also indicated. The inserted (right-handed) space-fixed axes illustrate the Tait-Bryan angles $\alpha_x, \alpha_y, \alpha_z$ which are used to specify the peptide orientation Ω. In the notation $\Omega=(\alpha_x, \alpha_y, \alpha_z)$ used in Figs. 5 and 6, Ω denotes the orientation with respect to $\alpha_x=0$, $\alpha_y=0$, $\alpha_z=0$ shown above. (The conventional right-handed positive rotation angles are indicated by the curved arrows.)

(*NPT*) ensemble. The time evolution of the area per lipid, shown in Fig. 3, indicates that the system equilibrates within 3 ns. After equilibration the average area per POPG lipid molecule is 66.3 ± 1.4 Å^2. This value is rather different from

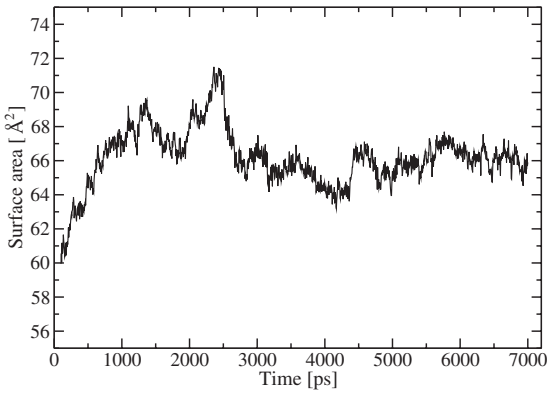

FIG. 3. Area per lipid head group for the POPG membrane as a function of time for a 7 ns simulation in the *NPT* ensemble.

the value 53.0 ± 0.6 Å^2 obtained using the GROMACS force field [31,33], but it is comparable with the corresponding value for the POPC bilayer (theoretical: 66.5 Å^2 [35]; and experimental: 68.3 Å^2 [36]). The average dimensions of the equilibrated POPG simulation box are $65.14 \times 65.14 \times 61.93$ Å^3. The mean distance d between phosphorus atoms in the two membrane leaflets is 36.3 Å.

(ii) Next we add another box of water molecules with one LFCinB peptide [protein data bank (PDB) code: 1lfc] [37] with ionized carboxyl group (C terminus) and amino groups (one N teminus and eight side chain groups) reflecting the typical protonation states at neutral *p*H in water. The LFCinB center of mass is positioned at a fixed distance from the membrane surface and at a fixed orientation. Subsequently, 22 sodium ions and 22 chlorine ions are added with each ion taking the place of a randomly chosen water molecule to create approximately a 0.1*M* physiological salt solution. In addition, eight chlorine counterions are added to neutralize the net charge of the peptide. The total number of chlorine ions in the combined system is then 30 and the number of sodium ions is 150. The total number of TIP3P water molecules is 10 492 and the water number density is 0.0334 molecules/Å^3, corresponding to a water mass density of 0.9983 g/cm^3. The total number of atoms in the system is 48 363.

After creating the system (POPG membrane with LFCinB and solvated ions) a set of 78 simulations for different LFCinB configurations with respect to the membrane (13 distances between the LFCinB center of mass and the membrane surface and 6 principal peptide orientations) is carried out. After energy minimization and preliminary equilibration for 500 ps in the in the *NVT* ensemble, the 78 LFCinB-POPG systems are equilibrated for 3 ns in the *NPT* ensemble. During equilibration, the area per lipid remained close, within the error bars, to the POPG system with (i) an average value of 66.3 ± 1.4 Å^2, indicating all of our simulation boxes are stable. Finally, for data collection, the 78 LFCinB-POPG systems are simulated for 4 ns in the *NVT* ensemble with the average area per lipid of 66.3 Å^2 (box dimensions of $64.02 \times 66.28 \times 117.37$ Å^3) and periodic boundary conditions.

IV. CONSTRUCTION OF PMF FOR PEPTIDE-MEMBRANE INTERACTION

In this section we summarize the methodology [3] for the calculations of the position and orientation PMF $W(z,\Omega)$, the position PMF $W(z)$, and the binding free energy for LFCinB peptide adsorption on a POPG membrane in a 0.1*M* salt solution. The distance z is the distance from the peptide center of mass to the membrane surface, defined as the surface containing the mean positions of the phosphorus atoms of the membrane upper leaflet. Since we restrict ourselves to six principal peptide orientations, it is convenient to specify the orientation by the three Tait-Bryan angles, $\Omega=(\alpha_x, \alpha_y, \alpha_z)$ (see Fig. 2). To carry out rotations of the peptide we use space-fixed axes x, y, and z with origin at the peptide center of mass (displaced for clarity in Fig. 2), x and y axes in the plane parallel to the membrane, and z axis perpendicular to

the membrane plane. The initial peptide orientation, (0, 0, 0), shown in Fig. 2 has the peptide backbone along y and the disulphide bond lying in the xy plane.

The orientational PMF $W(z,\Omega)$ has been evaluated for the following six principal orientations: $\Omega=(0,0,0)$, $(0,90°,0)$, $(0,180°,0)$, $(0,270°,0)$, $(90°,0,0)$, $(270°,0,0)$. As we see the first four correspond to "roll" rotations of the peptide around the y axis parallel to the membrane surface through angles $\alpha_y=0°,90°,180°,270°$, respectively, and the last two are "pitch" rotations about x axis of $\alpha_x=90°$ and 270°. The 90° pitch rotation corresponds to a configuration in which the peptide backbone is perpendicular to the membrane and the C and N termini are toward the surface. Because of the symmetry of the system we need not rotate the peptide around the z axis ("yaw" rotations). The peptide center of mass-membrane surface separation, z, ranges from 14 to 38 Å with increments of 2 Å. The simulation procedure is broken down into several stages:

(i) For a given orientation Ω the LFCinB peptide in the bulk is first separated from the membrane to a distance of 38 Å and is constrained in space. The POPG membrane center of mass is harmonically restrained with a spring with force constant 100 (kcal/mol)/Å^2. The system is equilibrated over 100 ps.

(ii) To create 78 simulation boxes for 13 different positions and 6 different orientations of the LFCinB-POPG system, harmonic restraint forces are applied to the all peptide backbone atoms and the anchor points of these restraints are then moved along the z direction for 100 ps for each step to decrease the center of mass mean distance by steps of 2 Å, keeping the orientation Ω and the membrane fixed at each step.

(iii) After creating the 78 initial systems, each of them is equilibrated for 500 ps in the *NVT* ensemble and then for 3 ns in the *NPT* ensemble. During this equilibration (and during data collection) the POPG membrane center of mass and the LFCinB peptide are harmonically restrained. To restrain the peptide and its orientation we use harmonic springs coupled to the three carbon C_α backbone atoms of Cys 3, Cys 20, and Pro 16. All spring constants are 100 (kcal/mol)/Å^2. The peptide center of mass and orientation move only very little (i.e., of the order of 0.01 Å) from the positions as generated by the steps in (ii).

(iv) The instantaneous restraint forces are computed during 4 ns trajectories in the *NVT* ensemble for each of the 78 system configurations with sampling interval of 0.2 ps and averaged to obtain the mean force $\bar{F}(z,\Omega)=-\bar{F}^{res}(z,\Omega)$ for each center of mass mean position (which we still call z). The PMF $W(z,\Omega)$ is calculated from $\bar{F}(z,\Omega)$ using Eq. (1), where integration over the z coordinate is performed using the trapezoidal rule.

The MD simulations of the forces acting on LFCinB and the calculations of the six independent profiles $W(z,\Omega)$ took about 500 000 cpu hours. $W(z)$ is obtained from $W(z,\Omega)$ using Eq. (2); for each value of z, we perform an unweighted average of the six simulated values of $\exp[-\beta W(z,\Omega)]$ to obtain $\exp[-\beta W(z)]$.

V. RESULTS

A. Ion-water-lipid complexes and counterion release from POPG membrane

Interaction of sodium ions with neutral and anionic phospholipids leads to the formation of Na^+-lipid and lipid-Na^+-lipid complexes, known as "ion bonds" and "salt bridges," respectively, which stabilize the membrane by reducing lipid-lipid repulsion [31,38]. Here we investigate the effect of the LFCinB proximity on the number of Na^+ counterions involved in the formation of such complexes with the anionic POPG lipids in our model membrane. During our test investigation of the PMF $W(r)$ for a Na^+-Cl^- ion pair, with r as the pair separation, we found [3] that the solvent-separated solute pair (SSSP) states, where a water molecule is shared between two ions, are more stable than the contact solute pairs (CSPs). Analyzing the results for the POPG membrane we find qualitatively the same effect, i.e., that solvent-separated ion-lipid pairs and salt bridges are more favorable compared to contact ion-lipid pairs and salt bridges without separating water molecules. We name these complexes SSSP and CSP, respectively, by analogy with the ion Na^+-Cl^- pairs in water. Therefore for our system we define the existence of an ion bond when any lipid head group oxygen is found within 3.5 Å of a Na^+ ion (the CSP state) or within 6.0 Å of Na^+ (the SSSP state). In addition we define the existence of salt bridges when at least two lipids and a Na^+ ion bind to each other through these extended ion bonds. When the distance between the LFCinB peptide and the phosphate plane is between 28 and 38 Å, we find, on average, that 81% (±2%) of the 128 Na^+ counterions are involved in ion bond formation with 54% (of 128 ions) in the SSSP states and only 27% (of 128 ions) in the CSP states. For POPG there are four types of relevant oxygens: (1) two OH oxygens each with the partial charge of $-0.66e$ in the CHARMM force field, (2) two equivalent phosphate oxygens with charge of $-0.78e$, (3) four ester oxygens (two ester oxygen of the phosphate group with charge of $-0.57e$ and another two with charge of $-0.34e$ near the carbonyl groups), and (4) two carbonyl oxygens with charge of $-0.52e$. The relative distributions of CSP ion bonds with oxygen types (1)–(4) are 21%, 57%, 6%, and 16% of the total, respectively, and the distributions of SSSP ion bonds are 23%, 30%, 27%, and 20%, respectively. The statistical analysis also shows that on average about 0.3 counterions are forming ion bonds (of both types) with each phosphate oxygen and about 0.15 ions are forming ion bonds with each of the other three types of oxygen. On average there are 240 ion-lipid "pairs" (per 128 POPG lipids). The percentages of the 128 Na^+ counterions "binding" to one, two, three, and four lipids are 20%, 27%, 23%, and 11%, respectively. Excluding ions "bound" to only one lipid, we have 61% of the Na^+ counterions participating in the formation of salt bridges between lipids.

To characterize the release of Na^+ ions from bound states with lipids upon peptide-membrane binding, we show in Fig. 4 the average total number of CSP and SSSP bound counterions near the upper leaflet of the POPG membrane averaged over a 4 ns simulation for the peptide orientation Ω

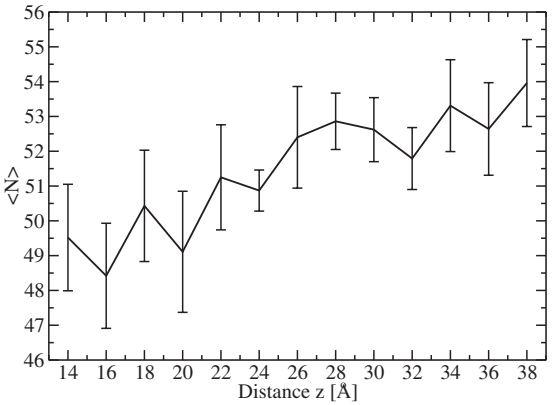

FIG. 4. The average number $\langle N \rangle$ of sodium counterions binding to the upper leaflet of the POPG membrane averaged over a 4 ns simulation for the peptide orientation $\Omega=(0,270°,0)$. z is the distance between the LFCinB center of mass and the phosphate plane of the upper leaflet of the POPG membrane.

$=(0,270°,0)$ versus peptide-membrane separation. We find that the LFCinB when bound at the PMF minimum distance (i.e., $\approx$16 Å) decreases the number of bound counterions $\langle N \rangle$, on average, by 5.0 ± 1.5 Na^+ ions compared to when LFCinB is in the bulk solution. Most of the released Na^+ ions belong to the SSSP state. We present here only the results for the LFCinB orientation with the minimum energy profile. The results for the average total number of bound counterions with different peptide orientations exhibit the same qualitative behavior.

Using the all-atom CHARMM27 force field [27] we observe that bound Na^+ ions show qualitatively different salt bridge formation, mostly through the SSSP states, in contrast to CSP states which were obtained using a GROMACS force-field MD simulation [31,33]. The latter work reported that 63% of the Na^+ counterions participate in CSP ion bond formation compared to 27% Na^+ counterions obtained from our simulations. These differences are consistent with earlier results which show that MD predictions are force-field dependent and that the qualitative difference depends in the nature of the force fields [39–41].

B. Binding affinity of LFCinB to charged POPG membrane

Figures 5 and 6 show the LFCinB-POPG PMFs $W(z,\Omega)$ from the simulation. For clarity, in Fig. 5 we display $W(z,\Omega)$ for the four orientations Ω in which the peptide backbone is parallel to the membrane and in Fig. 6 $W(z,\Omega)$ is given for the two peptide orientations in which the peptide backbone is perpendicular to the membrane. We find, as displayed in Fig. 5, that the PMF for $\Omega=(0,270°,0)$ has the minimum energy, in which the peptide backbone is parallel to the membrane and the side facing the membrane contains most of the basic residues. The PMF minima are about −7.0 kcal/mol deep for this orientation, and thus the charged POPG membrane forms a relatively strong binding complex with LFCinB compared to that with a neutral POPC membrane [with a $W(z,\Omega)$ minimum of −2.4 kcal/mol]. The least attractive profile with $\Omega=(270°,0,0)$, shown in Fig. 6, has the peptide

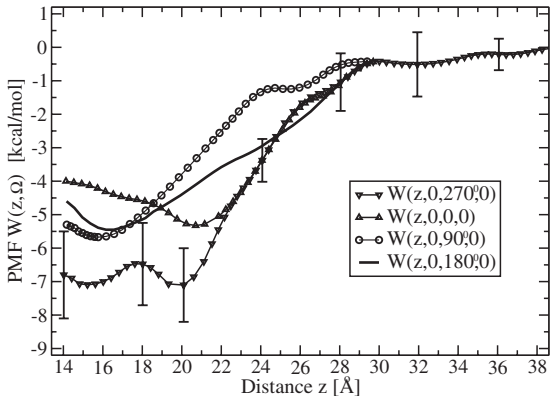

FIG. 5. PMF $W(z,\Omega)$ for LFCinB-POPG system for four peptide orientations Ω in which the peptide backbone is parallel to the membrane. z is the distance between the LFCinB center of mass and the phosphate plane of the upper leaflet of the POPG membrane. The notation $\Omega=(\alpha_x,\alpha_y,\alpha_z)$ is explained in the caption to Fig. 2. LFCinB with orientation $\Omega=(0,270°,0)$ has the minimum energy profile with the side facing the membrane containing most of the aromatic residues. Each data point represents the mean of eight 0.5 ns simulations of $W(z,\Omega)$, and the error bars represent the standard deviation obtained from the dispersion among the eight. The curves for the perpendicular orientations simulated are shown separately in Fig. 6.

backbone perpendicular to the membrane with C and N termini outward the surface. The curves for the other orientations simulated [i.e., $\Omega=(0,0,0)$, $(0,180°,0)$, $(0,270°,0)$, and $(270°,0,0)$] lie between those shown, as illustrated in Figs. 5 and 6.

To investigate the binding affinity for the peptide with Eqs. (4) and (3) we need to determine the binding geometry

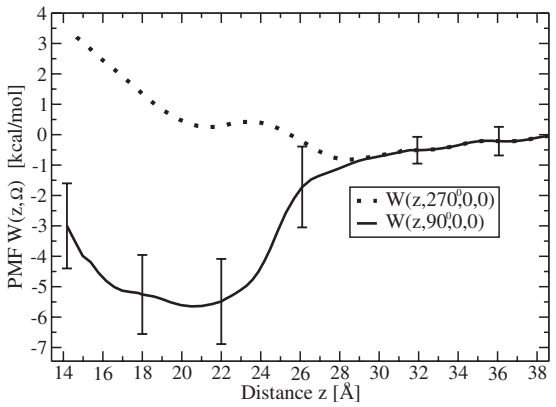

FIG. 6. PMF $W(z,\Omega)$ for LFCinB-POPG system for two peptide orientations Ω in which the peptide backbone is perpendicular to the membrane. z is the distance between the LFCinB center of mass and the phosphates plane of the upper leaflet of the POPG membrane. The notation $\Omega=(\alpha_x,\alpha_y,\alpha_z)$ is explained in the caption to Fig. 2. The least attractive (here purely repulsive) profile with $\Omega=(270°,0,0)$ has the C and N termini facing outward from the membrane surface. Each data point represents the mean of eight 0.5 ns simulations of $W(z,\Omega)$ and the error bars represent the standard deviation obtained from the dispersion among the eight. The curves for the parallel orientations simulated are shown separately in Fig. 5.

parameters for the system, l' and l, in the same way as was done in [3] with the POPC membrane. Analysis of the dimensions of the components of the system shows that the peptide can be represented by a spherical macroion with "effective" radius $a \approx 10$ Å and a POPG lipid head group with effective radius $b \approx 4$ Å. As a result, l' can be estimated from the radii of the peptide a and lipid head groups b, as $l' = a + b = 14$ Å. When analyzing the "restraint" forces $F^{res}(z,\Omega)$, we find that $\bar{F}(z,\Omega) \approx 0$ for $z > 36$ Å, and therefore peptides are considered to be bound within 36 Å (i.e., $l = 36$ Å). Using Eqs. (3) and (4) we find an adsorption free energy $\Delta G^0 = -5.37 \pm 1.25$ kcal/mol. The binding is relatively strong compared to the adsorption free energy of $\Delta G^0 = -1.05$ kcal/mol for a neutral POPC membrane [3]. Expressed in the terms of the forces involved, from the slopes in Fig. 6 we find the maximum average attractive force to be about 0.83 (kcal/mol)/Å or 58 pN, which is almost three times larger than that for the neutral membrane.

VI. ANALYSIS

A. LFCinB-POPG PMF from Poisson-Boltzmann theory

To analyze the nature of LFCinB-POPG interactions and to determine the contribution of the release of bound counterions to the peptide adsorption it is useful to decompose the adsorption free energy profile $W(z)$ into enthalpic $[\Delta H(z)]$ and entropic $[-T\Delta S(z)]$ components. As previously noted, the evaluation of $\Delta H(z)$ [Eq. (6)], performed in [3], is based on an assumption that the term $\beta[\partial W(z,\Omega)/\partial\beta]$ is small and can be neglected. Since this term is essentially an entropy term, $T\Delta S(z,\Omega)$, i.e., a change in the entropy at a fixed peptide orientation Ω, one cannot consider it to be small in the LFCinB-POPG system for the following reason. It has been shown that the interaction of LFCinB with the charged POPG membrane leads to a decrease in the number of counterions bound to the membrane (see Fig. 4) and hence W can have a substantial entropic component. (The assumption was justified for the case considered in [3], i.e., the LFCinB-POPC system, since the neutral POPC membrane does not require counterions and the LFCinB counterions can only be redistributed around LFCinB during adsorption to the POPC membrane.)

The approach we use in this section is to derive an approximate analytical equation for $W(z)$ using Poisson-Boltzmann theory and then to decompose it into enthalpic and entropic contributions. PB theory is a mean-field theory relating the mean electric field to the mean ion charge densities. It seems reasonable to use PB theory since the major interactions in the LFCinB-POPG system with strongly charged components are the electrostatic ones. If the PMFs derived from PB theory and MD simulations are in reasonable agreement, one has some confidence in the additional results derived from PB theory.

The cationic LFCinB-anionic POPG membrane system can be represented as a sphere with effective radius a and a planar surface, bearing two different fixed surface charge densities $\sigma_+ > 0$ and $\sigma_- < 0$, respectively, in an aqueous solution having a uniform dielectric constant ε and that contains the monovalent countercoin and coin, with the ions treated as continuous charge distributions. The PB equation can be used to describe the electrostatic interactions in this system. However, even for this simplified geometry, the PB equation is very difficult to solve and it is necessary to further simplify the geometry of the system to obtain an analytical solution. The simplest relevant geometry in our case is a geometry where a spherical surface charge distribution of the peptide is replaced by a planar charge distribution with the same surface density σ_+ but with the area similar in size to the opposite surface (both can be regarded as infinitely large planar surfaces). As a result, the simplified system consists of two oppositely charged parallel planes, separated by a distance D (see Fig. 1). The separation D is related to the distance z between the peptide center of mass and a negatively charged plane of POPG phosphate groups by $z = D + a$.

We assume that the electrolyte between the two charged planes is in thermodynamic equilibrium with a reservoir (both being at a fixed temperature T and with fixed overall system volume) containing a prescribed concentration c_0 for each of two monovalent ion species. In this case, the PB equation for the mean electric potential $\psi(\mathbf{r})$ at a point $\mathbf{r}$ in space between the two planes reduces to a nonlinear one-dimensional equation at any point z^* in the coordinate perpendicular to the planes (the running coordinate, with $z^* = 0$ chosen at the negative plane),

$$\phi''(z^*) = \kappa^2 \sinh \phi(z^*), \tag{7}$$

where $\phi(z^*) \equiv e\psi(z^*)/k_BT$, e is the proton charge, $\phi'(z^*) \equiv d\phi(z^*)/dz^*$, and (in esu) $\kappa = (D_{DH})^{-1} = \sqrt{8\pi D_B c_0}$ is the inverse Debye-Hückel screening length with D_B as the Bjerrum length, $D_B = e^2/\varepsilon k_B T$, for an aqueous solution of dielectric constant ε and c_0 as the ion number density in the reservoir where we choose $\phi = 0$. The boundary conditions relate the electric field $-\phi'$ at each of the two planes, separated by a distance D, to the charge densities, i.e., $\phi'(0) = -4\pi D_B \sigma_-/e = 2/D_{GC}^-$ and $\phi'(D) = 4\pi D_B \sigma_+/e = 2/D_{GC}^+$, where the Gouy-Chapman lengths D_{GC}^- and D_{GC}^+ for the corresponding surfaces are given by $D_{GC}^{\pm} = e/2\pi D_B|\sigma_\pm|$.

The solution of Eq. (7), the reduced electrostatic mean-field potential $\phi(z^*)$, allows evaluation of the difference in pressure, $\Delta P(D) = P_{in}(D) - P_{out}$, between that in the region between the surfaces $[P_{in}(D)]$ and that of the reservoir (P_{out}) at any plane-plane separation D. This pressure difference allows one to calculate the Helmholtz free energy change in the combined system, the charged planes system, and the reservoir as a function of D. The free energy change per area A_P is equal to a reversible work of the mean force $\bar{F}(D) = \Delta P(D) A_P$. When the two planes approach from infinity to the separation D the electrostatic free energy change per area A_P [or the PMF $W_{PB}(D)$] can be evaluated from

$$W_{PB}(D) = A_P \int_D^\infty \Delta P(D')dD', \tag{8}$$

where D' is the running separation between the two planes. We note here that we can neglect the change in the reservoir pressure P_{out} during the change in D and consequently the

Helmholtz free energy change $W_{PB}(D)$ can be assumed as essentially equal to the change in the Gibbs free energy $\Delta G(D)$. Similarly, the internal energy change $\Delta U(D)$ can be assumed equal to the enthalpy change $\Delta H(D)$.

From the PMF for the plane-plane geometry one can attempt to use the Deryaguin integration approximation [42] in order to get the PMF between a sphere and a planar surface. However, the Deryaguin approximation requires two conditions for its validity: (1) the radius of the sphere must be larger than the Debye-Hückel length and (2) the free energy must not go through extrema [43]. The second condition is clearly not met at the PMF minimum, so we did not use the Deryaguin integration approximation. Instead, to estimate the PMF for the sphere-plane geometry, we use the plane-plane geometry PMF [Eq. (8)] as described below.

We assume that the charged surfaces are rigid, ion-impenetrable, and with fixed charge densities. Real membranes have thermodynamic state-dependent fluidity and flexibility [44] and are ion penetrable. Their ionizable groups can change a surface charge with a corresponding change in surface potential. These complex considerations require solving the nonlinear PB equation with complicated boundary conditions (see review in [45]). Therefore, investigating model systems using MD simulations can elucidate the complex behavior of biological membranes and determine how well PB theory with simplified boundary conditions can explain the results.

Simple general closed form solutions for the PB equation exist only for the linearized approximation which is valid for $|\phi(z^*)| \ll 1$. This condition is usually satisfied in the limit of high salt concentration and at low surface potential [46]. The conditions in our simulations involve low salt concentration and highly asymmetric surface charge densities. Normally, this requires solving the nonlinear PB equation numerically [47]; however, for a few cases an analytical solution can be evaluated for the pressure $\Delta P(D)$ as a function of surface charge densities, salt concentration c_0, and surface separation D [48]. Another simplified case of two oppositely charged surfaces with no added salt and with only one type of counterion was considered in [49]. Below we will use analytical solutions, derived for the asymmetric PB models from [48,49] for two oppositely charged surfaces, to estimate the electrostatic free energy profile $W_{PB}(z)$ using Eq. (8), where the arbitrary surface area A_P is replaced by the area of an effective peptide surface exposed to the membrane counterions.

In the limit of low salt concentration ($D_{DH} \gg D_{GC}$) but for the plane-plane separation sufficiently large, $D > D_{DH}$, the pressure $\Delta P(D)$ between the interacting surfaces can be evaluated as [48]

$$\Delta P(D) \simeq -\frac{8k_BT}{\pi D_B D_{DH}^2} e^{-D/D_{DH}} = -64 c_0 k_B T e^{-D/D_{DH}}. \quad (9)$$

This expression is used in [48] for the case of a small difference between $|\sigma_-|$ and $|\sigma_+|$ and is independent of $\sigma_\pm$. But at a distance from a charged surface greater than several D_{GC} (in the limit of low salt concentration, when the initial surface screening is determined by the Gouy-Chapman length) the surface is relatively well screened and the further decay of the electric field depends only on the Debye-Hückel screening length, i.e., does not depend on the surface charge density. Thus the pressure difference, which can be determined by the electric field strength at the approximate midplane between the two surfaces [or more precisely at the point where $c_1(z^*)=c_2(z^*)=c_0$], decays exponentially at $D \gg D_{GC}^+ + D_{GC}^-$ (i.e., at $D > D_{DH}$) for arbitrary values of the surface charge densities within the limit of low salt concentration and use of Eq. (9) is justified.

Since for our membrane-peptide system we have $\sigma_- = -(1/66.3)\ e/\text{Å}^2 = -0.24\ \text{C/m}^2$, $\sigma_+ = (1/157)\ e/\text{Å}^2 = 0.10\ \text{C/m}^2$ and the Bjerrum length for the TIP3P water dielectric constant $\varepsilon \approx 95$ at $T=310$ K [50,51] is $D_B = 5.7$ Å, the corresponding Gouy-Chapman lengths are $D_{GC}^- = 1.9$ Å and $D_{GC}^+ = 4.4$ Å, respectively. These values are small compared to the Debye-Hückel screening length $D_{DH} = 10.0$ Å at $c_0 = 7 \times 10^{-5}$ Å$^{-3} \approx 0.1M$ at 310 K, and thus our conditions satisfy the limit of low salt concentration. Therefore, for $D > D_{DH}$ (i.e., for $D > 10$ Å) we can use Eq. (9) to estimate the pressure.

As the two charged surfaces approach each other, their original counterion distributions overlap. Being exposed to the electric field of the not completely screened opposite surfaces, the counterions from the overlapping tails of each distribution entropically prefer to escape to the reservoir rather than being squeezed by the increased field. For smaller separations, $D < D_{DH}$, and for the case, $|\sigma_-| \neq |\sigma_+|$, the counterions of the plane with a smaller $|\sigma|$ (here σ_+) can completely escape to the reservoir when the two surfaces come close enough. From this point, there is no further counterion escape at smaller separations since this would result in the plane-plane system having a net charge. For this specific case of one unscreened surface and the other partially screened, an exact analytical solution to the nonlinear PB equation has been obtained [49] and the pressure evaluated. Since there is no other "good" analytical solution for the PB equation in the region $D < D_{DH}$, we will use the pressure dependence from [49] in the entire region $D < D_{DH}$. This will slightly overestimate the attractive force between the two surfaces for larger separations within this region as the degree of surface screening remains unchanged for the model described in [49]. The relation between the pressure $\Delta P(D)$ and separation D for this model is

$$\Delta P(D) \simeq -\frac{k_BT}{8\pi D_B} E(D), \quad (10)$$

where for $E(D) > 0$, which corresponds to a negative pressure (i.e., attraction between the planes), $E(D)$ is defined implicitly by

$$E = \frac{4}{D_{GC}^- D_{GC}^+} - 2\left(\frac{1}{D_{GC}^-} - \frac{1}{D_{GC}^+}\right)\sqrt{E}\coth\left(\frac{\sqrt{E}D}{2}\right) \quad (11)$$

and, for $E(D) < 0$, when the pressure is repulsive, $E(D)$ satisfies

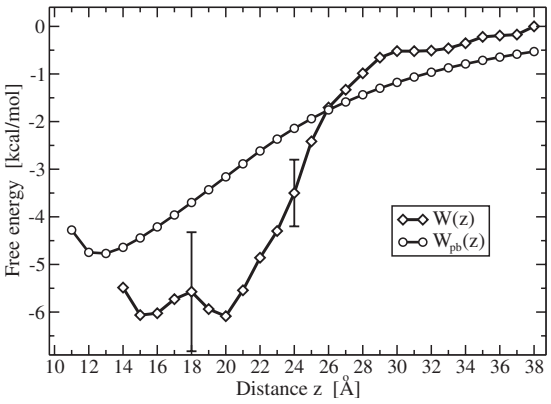

FIG. 7. The total free energy profile (PMF) $W(z)$ obtained from MD simulation and the theoretical electrostatic free energy profile from Poisson-Boltzmann theory, $W_{PB}(z)$, are shown. $W_{PB}(z)$ is calculated from PB theory using Eqs. (8)–(10). z is the distance between the LFCinB center of mass and the phosphates plane of the upper leaflet of the POPG membrane.

$$E = \frac{4}{D_{GC}^{-}D_{GC}^{+}} - 2\left(\frac{1}{D_{GC}^{-}} - \frac{1}{D_{GC}^{+}}\right)\sqrt{-E}\cot\left(\frac{\sqrt{-E}D}{2}\right). \tag{12}$$

An analytic expression for the quantity $E(D)$ can be calculated iteratively with the MAPLE10 software package using the first term on the right-hand side as starting value, with convergence after 11 steps for the choice of parameters (σ_+, σ_-, ε, and T) and separations used here. The crossover between attractive and repulsive pressures occurs when $E(D^*)=0$ at the separation $D^*=D_{GC}^{+}-D_{GC}^{-}$. At $D<D^*$ the repulsive forces between two oppositely charged surfaces originate from the squeezing of the remaining counterions in the gap between the two surfaces when the increasing osmotic pressure overcomes the electrostatic attraction between the surfaces [49].

Thus, for a qualitative estimation of the PB free energy profile [Eq. (8)] and its entropic and enthalpic components we use the pressure dependences [Eqs. (9) and (10)] in the regions above and below D_{DH}, respectively. To smoothly join the two solutions we switch from Eq. (9) to Eq. (10) at the separation when the two pressures are equal each other, i.e., at $D=11.5$ Å which is rather close to D_{DH}. Since we represent the peptide by a charged sphere with a radius a having its center at the distance $z=D+a$ from the negatively charged surface representing the membrane, the force on this sphere due to pressure $\Delta P(D)$ is $\pi a^2 \Delta P(D)$. This result, which neglects the pressure change along the curved sphere surface, allows us to estimate the area A_P of a planar surface roughly equivalent to the effective peptide surface as $A_P=\pi a^2$. In particular, for our system we have $A_P=314$ Å^2.

The electrostatic PB PMF $W_{PB}(z)$ calculated using Eq. (8) and with $z=D+a$, used to represent the separation, is plotted in Fig. 7 together with the orientation-averaged PMF $W(z)$ obtained from MD simulation of the POPG membrane interacting with LFCinB. The two curves are in relatively good agreement; perfect agreement is not expected since $W_{PB}(z)$ does not include attractive van der Waals interactions [3] and the peptide charge distribution is assumed to be uniform. In addition, the forces measured via MD simulation are slightly repulsive for the separation $z=14-15$ Å where LFCinB begins to overlap with the membrane lipid head groups. The presence of these groups, which are above the plane of charged phosphates (chosen to be $z=0$), alters the counterion distribution, but it is not taken into account in our simplified PB model. This is the reason the PB PMF begins to be repulsive only at separation $z=D_{GC}^{+}-D_{GC}^{-}+a=12.5$ Å. Despite these discrepancies, the simplified PB approach predicts a relatively good value of the PMF well depth for estimating the binding energy.

To decompose the PB PMF $W_{PB}(z)$ [Eq. (8)] into entropic $[-T\Delta S_{PB}(z)]$ and enthalpic $[\Delta H_{PB}(z)]$ [or internal energy $\Delta U_{PB}(z)$] contributions we need to take into account the temperature dependence of the water dielectric constant ε which is not explicitly present in Eqs. (9) and (10). This dependence should be included in our equations for the entropy calculation since polarization of a dielectric with high dielectric constant due to reorientation of permanent dipoles in an applied electric field (e.g., water) has a substantial entropic component. In a linear approximation for the temperature dependence (which is reasonably good for a small temperature interval of 10–20 K), using dielectric constant values for TIP3P water at two different temperatures [50,51], the temperature dependence of ε can be written as

$$\varepsilon(T) = \varepsilon_0 + \varepsilon'(T - T_0), \tag{13}$$

where $\varepsilon'=-0.34$ K^{-1} and $\varepsilon_0=95$ is the dielectric constant of TIP3P water at $T_0=310$ K.

The entropic contribution to $W_{PB}(z)$ with the dependence [Eq. (13)] incorporated into Eqs. (9) and (10) is then calculated using

$$-T\Delta S_{PB}(z) = T\frac{\partial W_{PB}(z)}{\partial T} = -\beta\frac{\partial W_{PB}(z)}{\partial \beta}. \tag{14}$$

This can be calculated analytically (with MAPLE) using the results for $W_{PB}(z)$.

The entropic contribution $[-T\Delta S_{PB}(z)]$ together with $W_{PB}(z)$ and $\Delta H_{PB}(z)$ calculated with Eq. (5) is shown in Fig. 8. We see that the PB electrostatic free energy profile essentially coincides with its entropy component, i.e., that the attraction of LFCinB to the POPG membrane, considered within PB theory, is of an almost entirely entropic nature. The entropy change, when two oppositely charged surfaces separated by an aqueous ion solution approach each other, is complex and consists of two major components. The first is the entropy of the ion distribution in the combined system. The second component is the entropy of the water solvent, a dielectric medium affected by the electric field between the two surfaces.

As noted before, when the tails of the two counterion distributions overlap, the electric field in this overlapping region increases while squeezing the screening counterions. Being in equilibrium with the reservoir the squeezed counterions from both distributions escape to the reservoir gaining entropy. As the separation between the two surfaces decreases, more and more ions leave the interplane gap increas-

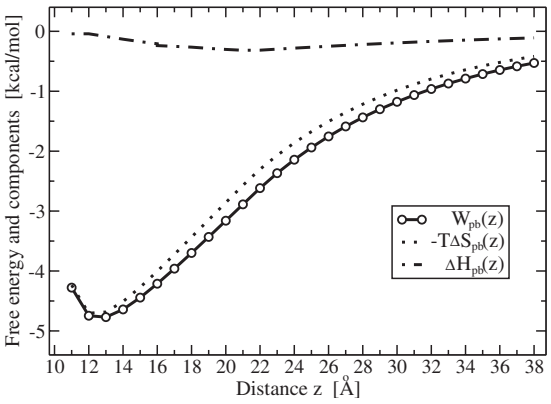

FIG. 8. PB electrostatic free energy profile $W_{PB}(z)$ and its decomposition using Eqs. (5) and (14) into entropy $-T\Delta S_{PB}(z)$ and enthalpy $\Delta H_{PB}(z)$ contributions. z is the distance between the LFCinB center of mass and a charged planar surface representing the POPG membrane.

ing the entropy of the overall system and hence producing the observed attraction. This process continues until the number of excess ions per unit area of a surface reaches the value $(|\sigma_+ + \sigma_-|/e$, decreasing from the initial value $(\sigma_+ + |\sigma_-|)/e$. At this point, the entropy of the ion distribution begins to decrease, raising the osmotic pressure, a component of the full pressure in the gap $\Delta P(D)$. These opposite tendencies in the ion distribution entropy change are related to the two different pressure dependences we use, Eqs. (9) and (10), respectively. The distance where we switch from the one to the other, $z \approx D_{DH}+a$, corresponds to the POPG-LFCinB separation where the number of bound membrane counterions shown in Fig. 4 stops decreasing. We will call the region beyond this distance the counterion release region.

The second major component of the system entropy is the entropy of the water between the two surfaces. Initially, when the two counterion distributions start to overlap, the entropy of the remaining water decreases due to the increase in the electric field in the overlap region that polarizes the water. This water entropy decrease slightly offsets the entropy gain due to the counterions escaping to the reservoir in the counterion release region, reducing the overall entropy contribution to $W_{PB}(z)$. At smaller plane-plane separations, in the region where we use the pressure dependence [Eq. (10)], the remaining counterions do not leave the gap, preventing further increase in the electric field and preventing further reduction in the water entropy due to increased polarization. However, decreasing the separation reduces the amount of polarized water between the charged surfaces, which increases the entropy of the combined system. This increase in water entropy is the major contributor to the electrostatic free energy decrease in the region $D^*+a<z<D_{DH}+a$, overcoming the decreasing ion distribution entropy, related to the osmotic pressure. Only at $z<D^*+a$ does the squeezed counterion entropy change become greater than the water entropy increase, leading to a rise of $W_{PB}(z)$.

The enthalpy $\Delta H_{PB}(z)$ [or equivalently the internal energy $\Delta U_{PB}(z)$] contribution to the PB PMF is negative (i.e., attractive) but negligible compared to $-T\Delta S_{PB}(z)$, being less than k_BT for our sphere-plane system. Thus, the entropy change, dominated first by the ion distribution entropy change in the counterion release region and then by the polarized dielectric entropy change, is the major contributor to the attraction between two oppositely charged surfaces.

Comparison of our LFCinB-POPG membrane results with our previous LFCinB-POPC membrane results [3] shows that the membrane-peptide interactions are dominated by contributions of different physical origins in the two cases. For the neutral POPC membrane the binding process is enthalpically driven, while for the charged POPG membrane, the adsorption free energy is dominated by the entropic contributions due to counterion release from the screening ion layers of the charged POPG membrane and the peptide and reducing the amount of polarized water between the two charged surfaces.

B. Application Poisson-Boltzmann theory to PG/PC mixed bilayer interacting with LFCinB

The results of Sec. VI A show that PB theory can be used to predict the interaction of the LFCinB peptide with the POPG membrane which is in a reasonable agreement with the results of MD simulations. In both cases we used the model membranes with the same surface charge density when all membrane lipid molecules are charged. In real bacterial membranes, there is a mixture of neutral and charged lipids. For most cytoplasmic bacterial membranes the charged lipids (mostly phosphatidylglycerols) comprise about 1/3 of all lipids [6]. Therefore a mixed PG/PC lipid bilayer with ratio of 1:2 (PG:PC) can be used as a model for the internal bacterial membrane interacting with the LFCinB antimicrobial peptide approximated by a charged sphere. The charge density of the mixed membrane (corresponding to D_{GC}=5.6 Å) in 0.1M salt solution still is in the limit of low salt concentration ($D_{DH} \gg D_{GC}$) and we can employ approximate solutions (9) and (10) from the nonlinear PB equation. For relatively large separations $D \gg D_{DH}$ between the charged surfaces, there may be no difference for the interactions of the peptide with the mixed PG/PC membrane and with the pure PG membrane, as the PB PMF, calculated at these separations using Eq. (9), does not depend on the surface charge densities. We expect some changes only in the region of smaller separations, $D \lesssim D_{DH}$, where the interaction between the partially screened surfaces (due to counterions having been released) is described by the pressure dependence [Eq. (10)]. Diluted by the neutral PC lipids, the surface charge density for the mixed PG/PC (1:2) membrane is $\sigma_- = -(1/199)\ e/\text{Å}^2 = -0.08\ \text{C/m}^2$, now slightly smaller in magnitude than that for the LFCinB peptide. Because of this, the electric field near the totally unscreened surface (now the membrane surface) is smaller than that for the pure PG membrane case. It is this field that determines the attractive component of the surface-surface interaction, and therefore, we can expect a lower attractive force for the separations $D < D_{DH}$ and a weaker PB PMF minimum.

The results of the calculation of the PB electrostatic free energy $W_{PB}(z)$ [Eq. (8)] and its entropic $[-T\Delta S_{PB}(z)]$ and enthalpic $[\Delta H_{PB}(z)]$ components for LFCinB interacting with the mixed PG/PC membrane are shown in Fig. 9. We

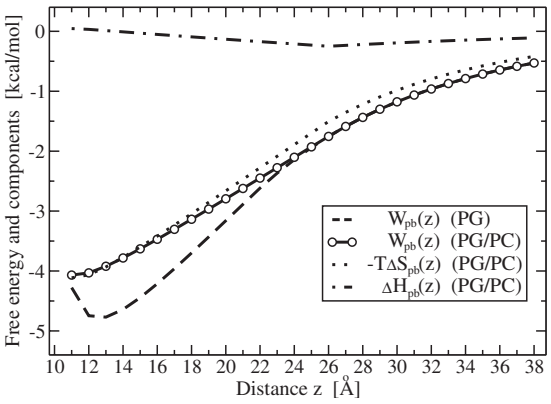

FIG. 9. PB electrostatic free energy profile $W_{PB}(z)$ and its decomposition into entropy $-T\Delta S_{PB}(z)$ and enthalpy $\Delta H_{PB}(z)$ contributions for the PG/PC membrane (1:2) interacting with a charged sphere representing the LFCinB peptide, obtained using expressions (5) and (14). The electrostatic PB PMF for the pure PG membrane is shown as well. z is the distance between the LFCinB center of mass and a charged planar surface representing the membrane.

use the approach described in Sec. VI A with the pressure dependences [Eqs. (9) and (10)]. Since relations (11) and (12) determining Eq. (10) were derived in [49] under the assumption $\sigma_+ < |\sigma_-|$ (i.e., $D^+_{GC} > D^-_{GC}$), and with the mixed PG/PC membrane we have $\sigma_+ > |\sigma_-|$, we need to change the sign in front of the second term in each of Eqs. (11) and (12). The switching point for calculating $\Delta P(D)$ from Eq. (9) or (10) now occurs at $D=16$ Å ($z=26$ Å).

As expected, we observe no significant change in the shape of the PMF $W_{PB}(z)$ and its components presented in Fig. 9 compared to the case of the pure POPG membrane (see Fig. 8). The PMF minimum is −4.1 kcal/mol, which is 0.7 kcal/mol higher than that for the pure POPG membrane (−4.8 kcal/mol). The new position of the minimum, where the crossover between an attractive and repulsive pressure occurs, is $z=a+D^*=a+D^-_{GC}-D^+_{GC}=11.2$ Å, shifted 1.3 Å toward the membrane compared to the pure POPG membrane case. Both of these changes are connected with the change in $|\sigma_-|$ which is now smaller and closer to σ_+. Thus, the remaining number of the excess counterions per unit area $(|\sigma_+ + \sigma_-|)/e$, which determines the repulsive force between the two charged surfaces, is much smaller. Experiments could be carried out to check our predictions for the binding affinity of LFCinB interacting with a charged POPG membrane, as well as with a mixed POPG/POPC membrane, using, for example, isothermal titration calorimetry.

VII. CONCLUSIONS

We use a variant of constrained MD with thermodynamic integration, which we have previously developed [3], to estimate from simulation the PMF for LFCinB interacting with a negatively charged POPG membrane. To estimate the standard free energy of adsorption ΔG^0 we calculate the binding constant K, which depends only on molecular characteristics and the actual state conditions, namely, the PMF $W(z)$, independent of the choice of standard state and independent of any additional adjustable parameters, such as an arbitrary cutoff of the binding region. Using this approach we predict the adsorption free energy to be $\Delta G^0 = -5.37 \pm 1.25$ kcal/mol and a corresponding maximum binding force of about 58 pN for LFCinB-POPG in a 100 mM salt solution at 310 K. The most favorable orientation of LFCinB $[\Omega=(0,270°,0)]$ has four of the basic residues facing the membrane, but as we see from Fig. 5 we have relatively weak dependence on orientation when the peptide backbone is parallel to the membrane. When the peptide is perpendicular to the membrane (see Fig. 6), strong orientation dependence of $W(z,\Omega)$ is observed. For the orientation with the ionized C and N termini toward membrane we see strong attraction, which has almost the same magnitude as for the orientation when the backbone is parallel to the membrane.

Our results can be summarized as follows. We first note that counterion release upon binding of LFCinB to the membrane shown in Fig. 4 supports the hypothesis that a possible mechanism of action for a CAP is to degrade the charged membrane by repelling cationic ions which normally function as cationic bridges between charged lipid head groups. After repelling cations from the membrane, the peptide itself may create ionic bonds with the charged lipid molecules. The entropy increase accompanying the counterion release from the electric double layers is one of the origins of the attraction between the strongly charged membrane and peptide. Another source of attraction is the entropy increase associated with the reduction in the amount of polarized water between the membrane and peptide charged surfaces. Our results from MD simulations are in good agreement with theoretical predictions based on analytical solutions of the nonlinear PB equation for systems with highly charged surfaces and with low bulk ion concentrations, where the Gouy-Chapman lengths are smaller than the Debye-Hückel screening length. We also carried out a PB analysis of LFCinB interacting with a mixed membrane (PG/PC=1/2) and found an attractive well depth about k_BT smaller than for a pure PG membrane.

From the point of view of selecting a peptide as a potential antimicrobial one, the relatively weak binding found for LFCinB-POPC [3] is encouraging since the POPC bilayer resembles idealized mammalian membranes, and it is required to find peptides which cause minimal damage to mammalian cells. Conversely, it is required to find peptides which interact strongly with bacterial-like (comparatively strongly charged) membranes (e.g., POPG, POPG/POPC) as LFCinB appears to do.

Further simulations of POPG and mixed POPC/POPG membrane-peptide systems, particularly in the contact region, will be useful because they will shed light on the mechanisms leading to peptide induced membrane disruption and membrane-peptide selectivity.

ACKNOWLEDGMENTS

We thank SHARCNET [25] for access to high-performance computing resources and NSERC [52] and AFMNet [53] of Canada for financial support.

[1] M. Zasloff, Nature (London) **415**, 389 (2002).
[2] H. Jenssen, P. Hammil, and R. E. Hancock, Clin. Microbiol. Rev. **19**, 491 (2006).
[3] V. Vivcharuk, B. Tomberli, I. S. Tolokh, and C. G. Gray, Phys. Rev. E **77**, 031913 (2008).
[4] H. J. Vogel, D. J. Shibili, W. Jing, E. M. Lohmeier-Vogel, R. F. Epand, and R. M. Epand, Biochem. Cell Biol. **80**, 49 (2002).
[5] P. F. Devaux, Biochemistry **30**, 1163 (1991).
[6] W. Dowhan, Annu. Rev. Biochem. **66**, 199 (1997).
[7] R. P. H. Huijbregts, A. I. P. M. de Kroon, and B. de Kruijff, Biochim. Biophys. Acta **1469**, 43 (2000).
[8] K. Matsuzaki, Biochim. Biophys. Acta **1462**, 1 (1999).
[9] K. Matsuzaki, K. Sugishita, M. Harada, N. Fujii, and K. Miyajima, Biochim. Biophys. Acta **1327**, 119 (1997).
[10] R. E. Hancock, Lancet **349**, 418 (1997).
[11] *Mammalian Host Defense Peptides*, edited by D. A. Devine and R. E. W. Hancock (Cambridge University Press, Cambridge, 2004).
[12] D. A. Pink, L. T. Hansen, T. A. Gill, B. E. Quinn, M. H. Jericho, and T. J. Beveridge, Langmuir **19**, 8852 (2003).
[13] S. O. Hagge, M. U. Hammer, A. Wiese, U. Seydel, and T. Gutsmann, BMC Biochem. **7**, 15 (2006).
[14] H. V. Westerhoff, D. Juretic, R. W. Hendler, and M. Zasloff, Proc. Natl. Acad. Sci. U.S.A. **86**, 6597 (1989).
[15] L. Yang, T. M. Weiss, R. I. Lehrer, and H. Huang, Biophys. J. **79**, 2002 (2000).
[16] C. B. Park, H. S. Kim, and S. C. Kim, Biochem. Biophys. Res. Commun. **244**, 253 (1998).
[17] R. M. Epand and H. J. Vogel, Biochim. Biophys. Acta **1462**, 11 (1999).
[18] K. A. Brogden, Nat. Rev. Microbiol. **3**, 238 (2005).
[19] *Free Energy Calculations*, edited by C. Chipot and A. Pohorille (Springer, Berlin, 2007).
[20] D. J. Tobias and C. L. Brooks III, Chem. Phys. Lett. **142**, 472 (1987).
[21] B. Roux and M. Karplus, Biophys. J. **59**, 961 (1991).
[22] G. Ciccotti, M. Ferrario, J. T. Hynes, and R. Kapral, Chem. Phys. **129**, 241 (1989).
[23] H. Shinto, S. Morisada, M. Miyahara, and K. Higashitani, J. Chem. Eng. Jpn. **36**, 57 (2003).
[24] E. Darve, in *Free Energy Calculations*, edited by C. Chipot and A. Pohorille (Springer, Berlin, 2007), p. 119.
[25] http://www.sharcnet.ca
[26] B. R. Brooks, R. E. Brucolleri, B. D. Olafson, D. J. States, S. Swaminathan, and M. Karplus, J. Comput. Chem. **4**, 187 (1983).
[27] A. D. MacKerell, D. Bashford, M. Bellot, R. L. Dunbrack, and J. Evanseek, J. Phys. Chem. B **102**, 3586 (1998).
[28] J. Kolafa and J. W. Perram, Mol. Simul. **9**, 351 (1992).
[29] J. P. Ryckaert, G. Ciccotti, and H. J. C. Berendsen, J. Comput. Phys. **23**, 327 (1977).
[30] W. L. Jorgensen, J. Chandrasekhar, J. D. Madura, R. W. Impey, and M. L. Klein, J. Chem. Phys. **79**, 926 (1983).
[31] W. Zhao, T. Rg, A. Gurtovenko, I. Vattulainen, and M. Karttunen, Biophys. J. **92**, 1114 (2007).
[32] http://www.apmaths.uwo.ca/mkarttu/downloads.shtml
[33] O. Berger, O. Edholm, and F. Jahnig, Biophys. J. **72**, 2002 (1997).
[34] I. Pascher, S. Sundell, K. Harlos, and H. Eibl, Biochim. Biophys. Acta **896**, 77 (1987).
[35] S. A. Pandit, S. W. Chiu, E. Jakobsson, A. Grama, and H. L. Scott, Biophys. J. **92**, 920 (2007).
[36] N. Kucerka, S. Tristram-Nagle, and J. F. Nagle, J. Membr. Biol. **208**, 193 (2005).
[37] http://www.rcsb.org
[38] S. A. Pandit, D. Bostick, and M. L. Berkovitz, Biophys. J. **85**, 3120 (2003).
[39] A. A. Gurtovenko, J. Chem. Phys. **122**, 244902 (2005).
[40] R. A. Bockmann, A. Hac, T. Heimburg, and H. Grubmuller, Biophys. J. **85**, 1647 (2003).
[41] S. K. Kandasamy and R. G. Larson, J. Chem. Phys. **125**, 074901 (2006).
[42] J. Israelachvili, *Intermolecular and Surface Forces*, 2nd ed. (Academic Press, London, 1997).
[43] E. Barouch, J. Matijevic, and V. A. Parsegian, J. Chem. Soc., Faraday Trans. 1 **82**, 2801 (1986).
[44] T. Ichikawa, in *New Colloid and Surface Science Research*, edited by L. V. Schwartz (Nova Science, New York, 2007), p. 197.
[45] D. Andelman, in *Handbook of Physics of Biological Systems*, edited by R. Lipowsky and E. Sackman (Elsevier Science, Amsterdam, 1995), Vol. 1, Chap. 12, p. 603.
[46] V. A. Parsegian and D. Gingell, Biophys. J. **12**, 1192 (1972).
[47] S. H. Behrens and M. Borkovec, Phys. Rev. E **60**, 7040 (1999).
[48] D. Ben-Yaakov, Y. Burak, D. Andelman, and S. A. Safran, EPL **79**, 48002 (2007).
[49] A. Lau and P. Pincus, Eur. Phys. J. B **10**, 175 (1999).
[50] H. A. Stern and S. E. Feller, J. Chem. Phys. **118**, 3401 (2003).
[51] P. Hochtl, S. Boresch, W. Bitomsky, and O. Steinhauser, J. Chem. Phys. **109**, 4927 (1998).
[52] http://www.nserc-crsng.gc.ca
[53] http://www.afmnet.ca